A&A 534, A81 (2011)
DOI: 10.1051/0004-6361/201116950


Astronomy & Astrophysics

# Dust-obscured star formation and the contribution of galaxies escaping UV/optical color selections at $z \sim 2$

L. Riguccini[1], E. Le Floc'h[1], O. Ilbert[2], H. Aussel[1], M. Salvato[3], P. Capak[4], H. McCracken[5], J. Kartaltepe[6], D. Sanders[7], and N. Scoville[4]

[1] Laboratoire AIM, CEA/DSM-CNRS-Université Paris Diderot, IRFU/Service d'Astrophysique, Bât. 709, CEA-Saclay, 91191 Gif-sur-Yvette Cedex, France
e-mail: [laurie.riguccini,emeric.lefloch]@cea.fr
[2] Laboratoire d'Astrophysique de Marseille, BP 8, Traverse du Siphon, 13376 Marseille Cedex 12, France
[3] Max-Planck-Institute für Plasma Physics, Boltzmann Strasse 2, 85748 Garching, Germany
[4] California Institute of Technology, MC 105-24, 1200 East California Boulevard, Pasadena, CA 91125, USA
[5] Institut d'Astrophysique de Paris, UMR7095 CNRS, Université Pierre et Marie Curie, 98bis boulevard Arago, 75014 Paris, France
[6] National Optical Astronomy Observatory, 950 N. Cherry Ave., Tucson, AZ, 85719, USA
[7] Institute for Astronomy, 2680 Woodlawn Dr., University of Hawaii, Honolulu, HI 96822, USA

Received 24 March 2011 / Accepted 31 May 2011

**ABSTRACT**

*Context.* A substantial amount of the stellar mass growth across cosmic time occurred within dust-enshrouded environments. So far, identification of complete samples of distant star-forming galaxies from the short wavelength range has been strongly biased by the effect of dust extinction. Nevertheless, the exact amount of star-forming activity that took place in high-redshift dusty galaxies but that has currently been missed by optical surveys has barely been explored.

*Aims.* Our goal is to determine the number of luminous star-forming galaxies at $1.5 \lesssim z \lesssim 3$ that are potentially missed by the traditional color selection techniques because of dust extinction. We also aim at quantifying the contribution of these sources to the IR luminosity and cosmic star formation density at high redshift.

*Methods.* We based our work on a sample of 24 $\mu$m sources brighter than 80 $\mu$Jy and taken from the *Spitzer* survey of the COSMOS field. Almost all of these sources have accurate photometric redshifts. We applied to this mid-IR selected sample the $BzK$ and $BM/BX$ criteria, as well as the selections of the IRAC peakers and the Optically-Faint IR-bright (OFIR) galaxies. We analyzed the fraction of sources identified with these techniques. We also computed 8 $\mu$m rest-frame luminosity from the 24 $\mu$m fluxes of our sources, and considering the relationships between $L_{8\ \mu\mathrm{m}}$ and $L_{\mathrm{Pa}_\alpha}$ and between $L_{8\ \mu\mathrm{m}}$ and $L_{\mathrm{IR}}$, we derived $\rho_{\mathrm{IR}}$ and then $\rho_{\mathrm{SFR}}$ for our MIPS sources.

*Results.* The $BzK$ criterion offers an almost complete (~90%) identification of the 24 $\mu$m sources at $1.4 < z < 2.5$. In contrast, the $BM/BX$ criterion misses 50% of the MIPS sources. We attribute this bias to the effect of extinction, which reddens the typical colors of galaxies. The contribution of these two selections to the IR luminosity density produced by all the sources brighter than 80 $\mu$Jy are on the same order. Moreover the criterion based on the presence of a stellar bump in their spectra (IRAC peakers) misses up to 40% of the IR luminosity density, while only 25% of the IR luminosity density at $z \sim 2$ is produced by OFIR galaxies characterized by extreme mid-IR to optical flux ratios.

*Conclusions.* Color selections of distant star-forming galaxies must be used with care given the substantial bias they can suffer. In particular, the effect of dust extinction strongly affects the completeness of identifications at the bright end of the bolometric luminosity function, which implies large and uncertain extrapolations to account for the contribution of dusty galaxies missed by these selections. In the context of forthcoming facilities that will operate at long wavelengths (e.g., JWST, ALMA, SAFARI, EVLA, SKA), this emphasizes the importance of minimizing the extinction biases when probing the activity of star formation in the early Universe.

**Key words.** galaxies: high-redshift – infrared: galaxies – cosmology: observations

## 1. Introduction

It is well established that the peak of star-forming activity in the Universe and the bulk of stellar mass assembly in galaxies occurred at $1 < z < 3$ (e.g., Madau et al. 1996; Steidel et al. 1999; Dickinson et al. 2003; Hopkins & Beacom 2006; Arnouts et al. 2007); however, the role and the contribution of the different processes that governed this build-up of stellar mass are still open questions. Improving our physical understanding of the population of star-forming galaxies that contributed to the growth of structures in the distant Universe thus remains a critical issue for modern extragalactic astrophysics.

To reach this goal, the broad variety of physical properties observed at high redshift usually implies using large and *complete* samples of galaxies mainly selected as a function of star formation rate (SFR) or stellar mass (see for instance Elbaz et al. 2007; Noeske et al. 2007; Ilbert et al. 2010). This requires systematic identification of sources with spectroscopic or photometric redshifts (e.g., Wolf et al. 2003; Fontana et al. 2004; Glazebrook et al. 2004; Cimatti et al. 2008). However, the determination of reliable spectroscopic redshifts for such large samples of distant galaxies is time-consuming because of the difficulty identifying emission or absorption lines with a high enough signal-to-noise ratio. Flux-limited optical selections are also dominated by populations of low-to-intermediate redshift sources, and they result in statistically small numbers of distant objects, while the limited coverage of spectroscopic surveys makes them sensitive to the cosmic variance effect.

Photometric redshifts, on the other hand, can suffer various systematics and contamination from catastrophic failures depending on the wavelength range and the number of bands they are based on, and their uncertainties can become significant in the case of distant galaxies.

To minimize these difficulties, various techniques based on single- or two-color criteria have been proposed to identify specific populations of galaxies in the early Universe. Among them, the first and best-known example is probably the selection of lyman break galaxies from the typical $U_nGR$ colors of sources at $z \sim 3$ (Steidel et al. 2003). Similarly, other techniques have been implemented to select galaxies at more intermediate redshifts ($1.5 \lesssim z \lesssim 3$) based on optical and infrared (IR) broad-band photometry. They include, for instance, the $BzK$ criterion (Daddi et al. 2004), the selection of $BM/BX$ sources (Steidel et al. 2004; Adelberger et al. 2004) and *distant red galaxies* (DRGs, Franx et al. 2003), the *extremely red objects* (EROs, Thompson et al. 1999) or the identification of massive sources through the shape of their stellar bump signature in the rest-frame near-infrared (Simpson & Eisenhardt 1999; Sawicki 2002; Huang et al. 2004). Each of these methods was designed to specifically isolate subpopulations of high-redshift galaxies based on a well-defined characteristic of their spectral energy distribution (SEDs, e.g., the blue color of their UV continuum, the red color of their evolved stellar populations, signatures of star formation reddened by dust, etc.). In this context they have been quite successfully used over the past ten years, and their high efficiency has dramatically revolutionized our understanding of galaxy formation in the early Universe.

The main advantage of these methods is their straightforward application, which requires only a few observing bands. Conversely, calibration over a restricted wavelength range also implies that they can hardly account for the overall diversity of galaxy properties at high redshift, making the use of these techniques perfidious beyond the scope for which they were originally defined. In particular, it is known that observations at rest-frame UV/optical wavelengths can be strongly affected by extinction. These techniques could thus suffer from biases due to the effect of dust, especially at the bright end of the bolometric luminosity function (LF) of star-forming galaxies where the contribution of dust-enshrouded star formation becomes dominant. Indeed, observations of the deep Universe taken with the *Spitzer* Space Telescope have revealed a high-redshift population of dusty luminous sources still almost invisible at shorter wavelengths, hence escaping the traditional UV/optical selections (Houck et al. 2005; Dey et al. 2008). What is the amount of star formation density produced at high redshift by these highly obscured sources? To what extent do galaxies currently missed by the standard color selection techniques contribute to the growth of stellar mass?

Over the last decades, observations in the mid- and far-infrared, as well as at submillimeter wavelengths, have enabled identification of a large number of luminous and dusty galaxies[1] throughout cosmic history and up to very large cosmological distances (e.g., Smail et al. 1997; Hughes et al. 1998; Aussel et al. 1999; Chary & Elbaz 2001; Blain et al. 2002; Le Floc'h et al. 2004; Marleau et al. 2004; Coppin et al. 2008; Capak et al. 2011). Detailed studies of these sources using multi-wavelength photometric and spectroscopic surveys have revealed that the bulk of their infrared luminosity comes from intense episodes of massive star formation, while they can also host powerful active nuclei triggered by nuclear accretion onto their central black holes (e.g., Yan et al. 2005; Pope et al. 2008; Menéndez-Delmestre et al. 2009; Hainline et al. 2009; Desai et al. 2009; Fadda et al. 2010). Although they have become rare objects in the present day, these LIRGs and ULIRGs were quite numerous in the past history of the Universe and dominated the comoving infrared energy density beyond $z \sim 0.5$, making up to 70% of star-forming activity at $z \sim 1$ (Le Floc'h et al. 2005). At higher redshift their contribution could be even greater (Caputi et al. 2007; Rodighiero et al. 2010), although the lack of sensitivity in mid-IR and far-IR experiments has prevented definitive conclusions on this issue. In fact, the respective contributions of dust-obscured and unobscured star formation to the growth of structures has been a debate for more than ten years (e.g. Adelberger & Steidel 2000). Whereas a general consensus recognizes that dusty and luminous star-forming galaxies played a critical role in driving massive galaxy evolution, it is also clear that at the peak of galaxy formation the faint-end slope of the UV LF was much steeper than observed in the local Universe, implying a larger contribution by faint galaxies to the cosmic star formation density (Reddy et al. 2008). Unfortunately, far-IR observations have not yet enabled direct probes of these faint high-redshift galaxies, while the characterization of luminous star-forming galaxies solely based on UV observations requires large extrapolations because of dust extinction. So far, it has therefore been difficult to reach consistent pictures from deep surveys performed at UV and far-IR wavelengths.

The goal of this paper is to address the fraction of luminous high-redshift galaxies that may be missed by the different color selection techniques commonly used to identify distant sources, and to quantify the impact of this bias by estimating the contribution of these objects to the IR luminosity and cosmic star formation density at $1.5 \lesssim z \lesssim 3$. We carried out this work using the deep 24 $\mu$m observations ($F_{24\,\mu\mathrm{m}} > 0.08$ mJy) of the COSMOS field (Scoville et al. 2007b) obtained with the MIPS instrument (Rieke et al. 2004) onboard the *Spitzer* Space Telescope. Among all facilities allowing the probe of dusty galaxies in the distant Universe (i.e. SCUBA, AzTEC, LABOCA, MIPS 70 and 160 $\mu$m, etc.), MIPS 24 $\mu$m observations provide one of the deepest sensitivity limits currently feasible up to $z \sim 2$–$3$. Furthermore, the deep optical/near-IR imaging, as well as the high-quality photometric redshifts obtained in the COSMOS field (Ilbert et al. 2009), have enabled a detailed characterization of the redshift distribution associated to the whole sample of 24 $\mu$m sources up to $z \sim 3$ (Le Floc'h et al. 2009), hence providing a complete and unbiased view of the population of dusty high-redshift sources selected at $F_{24\,\mu\mathrm{m}} > 0.08$ mJy. Taking advantage of the broad coverage of COSMOS to minimize the effect of cosmic variance, we applied the color criteria associated to four different selections of distant galaxies ($BzK$ & $BM/BX$ sources, IRAC peakers and Optically-Faint IR-bright (OFIR) objects), and we quantified the amount of high-redshift 24 $\mu$m sources missed by each of these techniques. Our data are described in Sect. 2, the criteria that we explored are presented in Sect. 3, and the corresponding subselections that we obtained based on the MIPS-detected COSMOS population are discussed in Sect. 4. In Sect. 5 we present the rest-frame 8 $\mu$m LF of the complete high-redshift MIPS sample, as well as the contribution of the subpopulations of galaxies respectively identified with the color selection techniques mentioned earlier. Our results are discussed in Sect. 6 and we finally present our conclusions in Sect. 7. Throughout this paper we assume a $\Lambda$CDM cosmology with $H_0 = 70$ km s$^{-1}$, $\Omega_\mathrm{m} = 0.3$, and $\Omega_\lambda = 0.7$. Magnitudes are

[1] These sources are referred to as luminous infrared galaxies (LIRGs: $10^{11}\ L_\odot < L_\mathrm{IR} < 10^{12}\ L_\odot$ with $L_\mathrm{IR} = L_{8-1000\,\mu\mathrm{m}}$) and ultra-luminous infrared galaxies (ULIRGs: $L_\mathrm{IR} > 10^{12}\ L_\odot$).

given in the AB system and the conversions between luminosities and star formation rates (SFRs) are computed assuming the initial mass function from Salpeter (1955).

## 2. The data

The sample of luminous star-forming galaxies used in this work was selected from the deep *Spitzer*/MIPS observations of the 2 deg$^2$ COSMOS field (Sanders et al. 2007) and it is based on the 24 $\mu$m source catalog obtained by Le Floc'h et al. (2009). COSMOS is the largest contiguous imaging survey ever undertaken with the HST (Scoville et al. 2007a) to a depth of $i^+ = 28.0$ [AB] ($5\sigma$ on an optimally extracted point source; Capak et al. 2007). The COSMOS field is located near the celestial equator to ensure visibility by all ground and spaced-based astronomical facilities. It is devoid of bright X-ray, UV, and radio foreground sources, and compared to other equatorial fields the Galactic extinction is remarkably low and uniform ($\langle E_{(B-V)} \rangle \simeq 0.02$). Extensive multiwavelength follow-ups with ground-based and spaced-based facilities have also been achieved with high-sensitivity imaging and spectroscopy spanning the entire spectrum from the X-ray to the radio (Hasinger et al. 2007; Schinnerer et al. 2007; Lilly et al. 2007; Elvis et al. 2009). In particular, deep UV-to-8 $\mu$m photometry was obtained over 30 different bands using narrow, medium, and broad-band filters (e.g., Taniguchi et al. 2007; Capak et al. 2007), while far-IR and submillimeter/millimeter observations were performed with various instruments such as MIPS onboard *Spitzer* (Sanders et al. 2007), PACS and SPIRE onboard *Herschel* (Lutz et al. 2011; Oliver et al., in prep.), SCUBA-2, AzTEC, MAMBO, and BOLOCAM (e.g., Bertoldi et al. 2007; Austermann et al. 2009).

While the 24 $\mu$m source catalog of COSMOS covers a total area of 2 deg$^2$, we restricted our sample to the field outside the regions contaminated by very bright or saturated objects where the photometry is less accurate. We also applied a conservative flux cut of 80 $\mu$Jy, corresponding to a completeness of ~90% in the source extraction performed by Le Floc'h et al. (2009). This led to a sample of 29 395 sources detected at 24 $\mu$m over an effective surface of 1.68 deg$^2$.

The counterparts of the MIPS-selected detections were identified following the same procedure as the one described by Le Floc'h et al. (2009). Given the much higher density of sources detected at optical wavelengths in COSMOS (Capak et al. 2007) than those detected with MIPS, a direct cross-correlation between the 24 $\mu$m-selected catalog and the optical observations could lead to several spurious associations with optically-detected galaxies randomly aligned close to the line of sight of the MIPS sources. Hence, we first cross-correlated the 24 $\mu$m data with the COSMOS $K_s$-band catalog of McCracken et al. (2010) to minimize the risk of wrong associations. The density of sources in this catalog is substantially lower than at optical wavelengths, while it is deep enough ($5\sigma$ for $K_s = 23.7$) to allow the identification of near-IR counterparts for most of the 24 $\mu$m detections in COSMOS (e.g., Le Floc'h et al. 2009). Also, the $K_s$-band observations were carried out under very good seeing conditions (~0.7″ at 2.2 $\mu$m), leading to a much narrower PSF than obtained in the other near-IR images of COSMOS (e.g., IRAC-3.6 $\mu$m) and allowing more robust identifications for blended sources. Our correlation between the 24 $\mu$m and $K_s$-band data was performed with a matching radius of 2″. Given the width of the 24 $\mu$m PSF ($FWMH \sim 6''$), this radius allowed us to identify most of the 24 $\mu$m sources while also minimizing the number of multiple matches. Similar to the results obtained by Le Floc'h et al. (2009), only 765 sources from the initial sample of 29 395 mid-IR objects could not be matched in the near-IR, while up to 84% sources from the MIPS catalog were identified with a clean and single $K_s$-band counterpart. For the rest of the sample (13%), two possible matches were found within the matching distance. For those cases we decided to keep the closest counterpart, as for most of them (~60%) the centroid was at least twice closer to the 24 $\mu$m source than the second possible match.

In a second step we correlated the list of these $K_s$-band identifications with a recently updated version of the $i^+$-band selected catalog of photometric redshifts from Ilbert et al. (2009) using a matching radius of 1″. Given the depth of the COSMOS $i^+$-band data (e.g., Capak et al. 2007) at the end, 1306 MIPS sources could not be matched at optical wavelengths, leading to the identification of optical counterparts and redshift determination for more than 95% of the initial 24 $\mu$m-selected sources. As part of this second cross-correlation, double optical matches were obtained for only ~1% of the $K_s$-band counterparts, underlying the robustness of our identification at these short wavelengths. For these few cases, we again kept the closest possible optical association. The catalog of Ilbert et al. (2009) includes the band-merged COSMOS photometry published by Capak et al. (2007), McCracken et al. (2010), and Ilbert et al. (2010) from the $U$-band to the IRAC 8 $\mu$m. Our cross-correlation thus yielded direct determination of optical/near-IR broad-band magnitudes for all selected galaxies. In particular, we considered the photometry in the $u^*$, $B_J$, $V_J$, $r^+$, $i^+$ and $z^+$ bands[2], where the 5-$\sigma$ magnitude limit reaches 26.5, 26.6, 26.5, 26.6, 26.1, and 25.1, respectively (Capak et al. 2007). Finally, Ilbert et al. (2009) also provide the identification of sources detected with XMM over COSMOS (e.g., Brusa et al. 2010, 2007; Salvato et al. 2009), which allowed us to systematically exclude the X-ray-detected AGNs from our final sample down to a flux limited $S_{0.5-2\,\mathrm{keV}} = 5 \times 10^{-16}$ erg cm$^{-2}$ s$^{-1}$ (less than 4%).

## 3. Photometric selection techniques

### 3.1. Optical and NIR color selections

#### 3.1.1. The *BzK* selection

Based on deep photometry obtained with $B$-band, $z$-band and $K$-band filters, Daddi et al. (2004) proposed a criterion for selecting star-forming galaxies in the redshift range of $1.4 < z < 2.5$: $BzK \equiv (z - K)_{AB} - (B - z)_{AB} > -0.2$. In the plane defined by $z - K$ as a function of $B - z$ (hereafter the $BzK$ diagram), the extinction vector obtained for the attenuation law of Calzetti et al. (2000) is parallel to the line characterized by $BzK = -0.2$ at $1.5 < z < 2.5$. Therefore this criterion offers the advantage of being mostly independent of dust obscuration.

The $B$-band, $z$-band, and $K$-band photometry used by Daddi et al. (2004) was based on the Bessel-$B$ and $K_s$ filters available at the VLT, as well as on the F850LP $z$-band filter of HST. On the other hand, our COSMOS photometry was determined through $B_J$ and $z^+$-band observations obtained at the Subaru Telescope and $K_s$-band data taken at CFHT (Capak et al. 2007; McCracken et al. 2010). In order to adapt the original $BzK$ criterion to the COSMOS data, we thus determined the evolution of the $BzK$ variable through the COSMOS filters as a function of redshift and with a set of star-forming galaxy templates similar

[2] In this work we also applied the systematic offsets inferred by Ilbert et al. (2009) to the COSMOS broad-band photometry when computing their photometric redshifts (see their Table 1).

to the library of SEDs used by Ilbert et al. (2009) for their catalog of photometric redshifts in COSMOS, and we compared this $BzK$ variable to the $BzK_o$ color initially defined by Daddi et al. (2004). The star-forming SEDs used by Ilbert et al. (2009) were generated with the stellar population synthesis model of Bruzual & Charlot (2003) assuming exponentially-declining star formation histories and starburst ages between 0.03 and 3 Gyr. In the redshift range of $1.4 < z < 2.5$ we found $BzK - BzK_o = 0.1$ mag with a very small dispersion driven by the choice of SED template. To apply the $BzK$ selection technique to the COSMOS survey we thus added a systematic offset of +0.1 mag to the initial criterion proposed by Daddi et al. (2004), leading to identification of star-forming $BzK$ galaxies with the color

$$BzK \geqslant -0.1. \quad (1)$$

#### 3.1.2. The *BM/BX* criteria

Another widely used selection of distant star-forming sources has been proposed by Steidel et al. (2004) and Adelberger et al. (2004) using UV/optical broad-band color selection techniques. Based on photometry obtained in the $U_n$, $G$, and $R$ bands and using the associated $U_n - G$ and $G - R$ colors, they defined two criteria referred to as the "BM" and "BX" selections to identify galaxies at $1.4 \leq z \leq 2.1$ and $1.9 \leq z \leq 2.7$, respectively.

At the wavelengths where these two selection techniques can be applied, the COSMOS observations were carried out at the CFHT and at the Subaru Telescope with the $u^*$, $g^+$ and $r^+$ filters (Capak et al. 2007), which differ substantially from the filters used by Steidel et al. (2004). As a result we were not able to adapt the initial $BM/BX$ selection to the COSMOS photometry by applying simple terms of color corrections and/or systematic offsets to our data. Following the approach proposed by Grazian et al. (2007), we considered a slightly modified version of the $BM/BX$ criterion using the $u^* - V_J$ and $V_J - i^+$ colors instead of the colors initially used by Adelberger et al. (2004). To determine the most appropriate color cuts for our $u^*V_Ji^{+\prime}$ diagram, we computed the evolution of color tracks followed by star-forming galaxies as a function of redshift, in a very similar way to the one employed by Adelberger et al. (2004) so as to ensure a selection of star-forming sources that is as close as possible to the original criterion. We used the SEDs of two starburst galaxies in the list of galaxy templates considered by Ilbert et al. (2009) for their analysis of the COSMOS photometric redshifts. These two SEDs were chosen as being the most representative templates of galaxies beyond $z \sim 1$ according to the SED fitting inferred by Ilbert et al. (2009). These two templates correspond to starburst models taken from (Bruzual & Charlot 2003, hereafter BC03) to which emission lines has been added to gain a better understanding of the COSMOS colors (for more details see Ilbert et al. 2009). Following Adelberger et al. (2004), we also took the effect of extinction into account by reddening each template up to $E(B - V) = 0.2$ assuming the attenuation curve of Calzetti et al. (2000).

The exact determination of our new selection is illustrated in Fig. 1. First we defined the lower and upper limits of our criterion on the $u^* - V_J$ color using the location of the galaxy tracks at $z = 1.5$ and $z = 2.8$, respectively:

$$\begin{aligned} u^* - V_J &> 0.52(V_J - i^+) - 0.1 \\ u^* - V_J &< 2.5(V_J - i^+) + 1.0. \end{aligned} \quad (2)$$

Second, we used a lower limit of −0.25 for the $V_J - i^+$ color. It is similar to the cut chosen by Grazian et al. (2007), although we note that its effect is negligible since very few sources are bluer than this limit. Finally, we imposed an upper limit on this second color so as to allow the selection of sources corresponding to the reddest templates of our diagram ($E(B - V) = 0.2$ mag):

$$u^* - V_J < -12.5(V_J - i^+) + 9.0. \quad (3)$$

Similar to what had been noticed by Adelberger et al. (2004), the galaxy tracks illustrated in Fig. 1 reveal an important degeneracy between the colors of low-redshift galaxies and more distant sources affected by dust extinction. The $V_J - i^+$ upper limit that we adopted corresponds to the compromise of allowing the selection of dusty galaxies while minimizing the contamination of sources at $z < 1$. As we see later in this section, this will have strong impact on the selection of luminous and dusty star-forming objects with $E(B-V) > 0.2$ using the $BM/BX$ technique. We did, however, keep a strict cut at $E(B - V) = 0.2$ to not alter the original $BM/BX$ criterion proposed by Adelberger et al. (2004).

To verify the robustness of our new color selection we overploted in Fig. 1 the observed colors of the $i^+$-band selected COSMOS galaxies with the aforementioned redshift cut of $z > 1.5$ (Capak et al. 2007; Ilbert et al. 2009). For clarity, only sources with $i^+ < 25$ are shown, to minimize the dispersion coming from photometric uncertainties. As expected from the SED tracks, we see that our criterion is generally well suited to identifying optically-selected star-forming galaxies at $1.5 < z < 2.8$. Out of the 28 141 $i^+$-band sources located in this redshift range and selected at $i^+ < 25$ from the photometric redshift catalog of Ilbert et al. (2009), 24 826 sources (i.e., 88%) satisfy our modified $BM/BX$ selection. Among the remaining objects that escape the selection, some are substantially affected by dust extinction, and their optical colors are thus redder than allowed by the criterion, while some others are characterized by photometric uncertainties moving them just outside of our $BM/BX$ selection box. Most of them, however, correspond to blue sources with photometric redshifts just above $z = 1.5$. Therefore the small incompleteness of our criterion mostly reflects the color degeneracy that appears at this redshift because of SED variations and dust extinction, as well as uncertainties affecting our photometric redshifts in the COSMOS field. Relaxing our lower limit on the $u^* - V_J$ to reduce this incompleteness by 12% would inevitably increase the fraction of contaminants from sources at $z < 1.5$.

#### 3.1.3. Distant "stellar-bump dominated" galaxies

After the successful launch of the *Spitzer* Space Telescope, the advent of deep surveys carried out with the IRAC instrument enabled a new approach to identifying distant star-forming galaxies, based on the rest-frame 1.6 $\mu$m bump produced by the $H^-$ opacity minimum in the atmospheres of cool stars (Simpson & Eisenhardt 1999; Sawicki 2002). At $1.5 < z < 3$, the signature of this stellar bump is shifted between 3 and 9 $\mu$m, and it reveals itself through specific colors across the IRAC bands. It allows identification of distant galaxies in a way that is less subject to extinction than are the optically-based selections discussed earlier.

Several selection techniques have been explored to apply this method to large galaxy samples. They involve either a direct fit of the IRAC fluxes with stellar templates (e.g., Sorba & Sawicki 2010), the use of two-color criteria (e.g., Papovich 2008; Huang et al. 2004, 2009), or the simple identification of the SED peak across the four IRAC channels (e.g., Lonsdale et al. 2009). For our current analysis we considered the selection introduced by Huang et al. (2004). It is based on the color

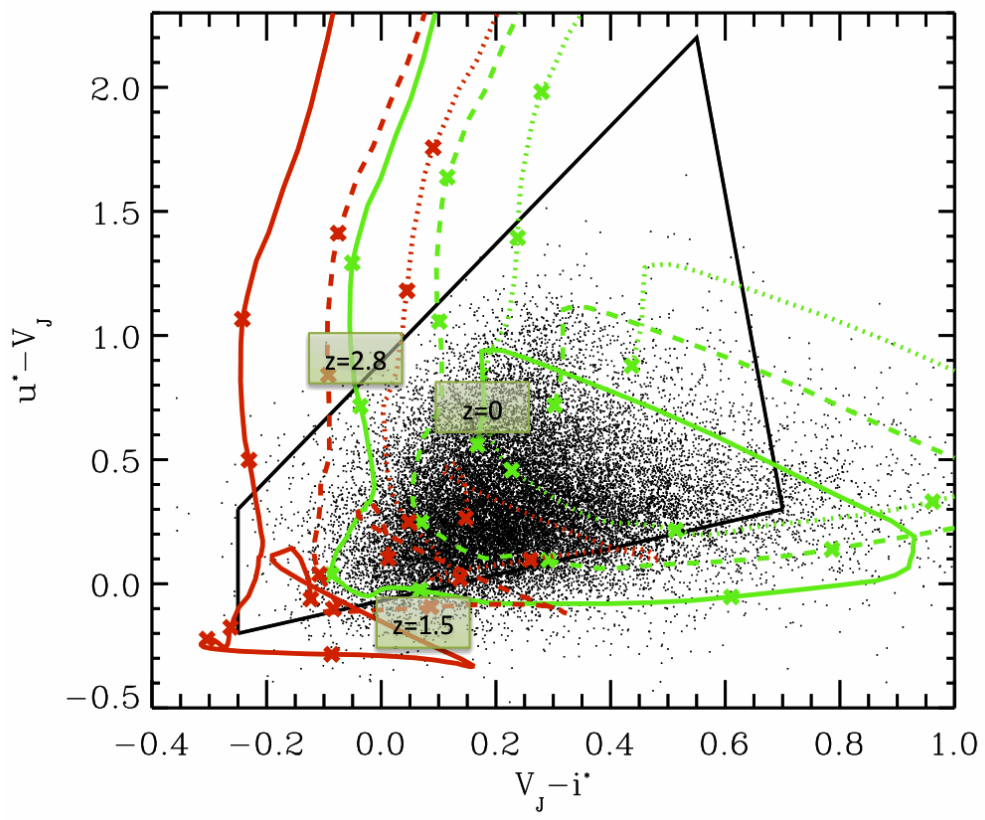


**Fig. 1.** Selection of galaxies at $1.5 < z < 2.8$ based on $u^* - V_J$ and $V_J - i^+$ colors. The galaxy tracks represented by the green and red solid curves correspond to the colors predicted as a function of redshift for two typical star-forming galaxy templates used by Ilbert et al. (2009) for determining of photometric redshifts in COSMOS. The dashed and dotted lines show the effect of dust extinction produced by $E(B-V) = 0.1$ and 0.2 assuming the law of Calzetti et al. (2000). The cross symbols along the tracks correspond to $z = 0$, 1, 1.5, 2, 2.8, and 3. The black solid lines show the limits of our modified $BM/BX$ criterion. The distribution of the optically-selected COSMOS galaxies at $1.5 < z < 2.8$ (black dots, limited for clarity to sources with $i^+ < 25$ and photometric uncertainties below 0.1 mag in $u^*$, $V_J$ and $i^+$) illustrates the high reliability of our color selection.

cuts $0.05 < [3.6] - [4.5] < 0.4$ and $-0.7 < [3.6] - [8.0] < 0.5$, where [3.6] denotes the AB magnitude in the 3.6 $\mu$m band (and likewise for the 4.5 and 8.0 $\mu$m bands). Extensive follow-up has confirmed the reliability of this criterion for selecting galaxies at $1.5 < z < 3$ (Huang et al. 2009; Desai et al. 2009). These sources are referred to as the IRAC peakers hereafter.

### 3.2. Selection of optically faint IR-bright sources at $z \sim 2$

While the selection techniques discussed in the previous section pertain by definition to sources primarily identified at optical and near-IR wavelengths, observations undertaken in the thermal infrared and the submillimeter have revealed several luminous galaxies associated with optical counterparts that are much fainter than the typical magnitude limits considered in the surveys of the distant Universe carried out in the visible ($I \sim 25$ mag AB, e.g., Hughes et al. 1998; Houck et al. 2005; Yan et al. 2005). Given the extreme IR-to-optical colors that result from these faint magnitudes at visible wavelengths, various criteria based on the mid-IR/optical flux ratio have thus been proposed for selecting dusty star-forming sources at $z > 1$. However, the relevance of the galaxy subsamples selected with this approach and their contribution with respect to the global population of high-redshift sources has barely been explored so far. Here we describe the selection technique that was proposed by Dey et al. (2008), based on the ratio between the 24 $\mu$m and the optical $R$-band flux densities. Using the *Spitzer* observations of the Bootes Field and the NOAO Deep Wide-Field Survey (NDWFS) they analyzed the population of 24 $\mu$m sources brighter than 0.3 mJy (i.e., the depth of the MIPS imaging in Bootes) and they defined a selection of dust-enshrouded high redshift sources[3] with the following criterion:

$$R - [24] \geqslant 7.4 \text{ mag (AB)} \quad (4)$$

where [24] refers to the AB magnitude measured in the MIPS-24 $\mu$m band[4]. Using spectroscopic follow-up performed with the IRS spectrograph onboard *Spitzer* and with the LRIS/DEIMOS instruments at the *Keck* telescopes, they have shown that their technique provides a reliable selection of dusty luminous galaxies at $1.5 < z < 3$, with a small fraction of contaminants from lower redshifts.

## 4. Application to the 24 $\mu$m selected galaxy populations in COSMOS

### 4.1. The optical/near-IR selections applied to the 24 $\mu$m galaxy population: associated redshift distributions

To quantify how the UV/optical selections of distant sources suffer from biases and incompleteness due to dust extinction,

[3] Referred to as "Dust-Obscured Galaxies" in their selection at $F_{24\ \mu m} > 0.3$ mJy.

[4] The relation given by Dey et al. (2008) uses the Vega system and it was converted following the MIPS Data Handbook: $[24](\text{Vega}) = -2.5 \times \log_{10} \frac{f_{24\ \mu m}(\text{Jy})}{7.14}$.

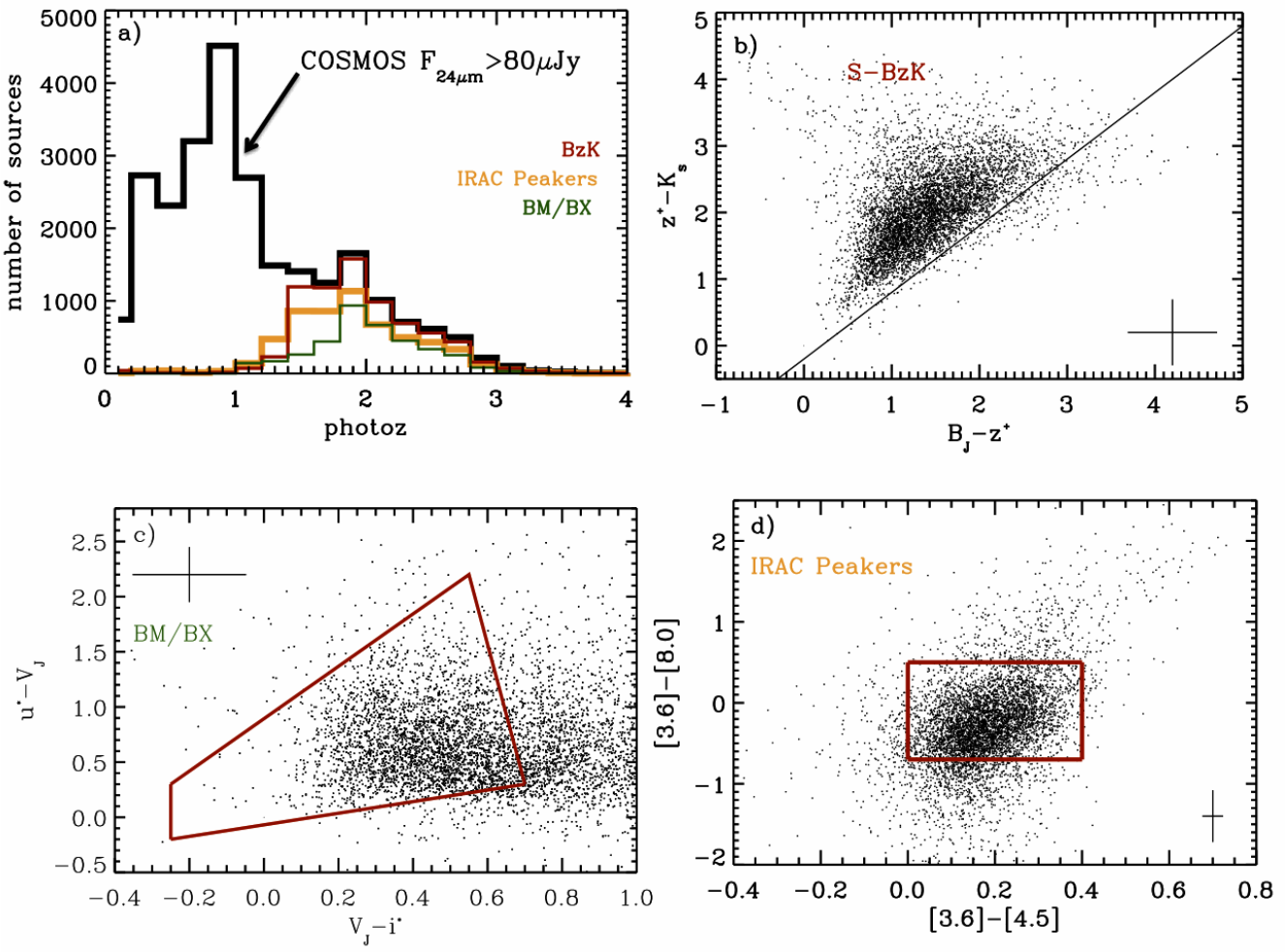


**Fig. 2. a)** Redshift distributions of the MIPS galaxies identified with the *BzK* (red), *BM*/*BX* (green), and IRAC peaker (orange) selection techniques, compared to the distribution obtained for the whole sample of COSMOS sources with $F_{24\ \mu m} > 0.08$ mJy (black solid histogram). **b)** The *BzK* color distribution of the MIPS galaxies identified at $1.4 < z < 2.5$ with the COSMOS photometric redshifts. The *BzK* star-forming sources ($S - BzK$) are identified above the diagonal solid line. **c)** Distribution of the $1.5 < z < 2.8$ MIPS galaxies in the $V_J - i^+$ versus $u^* - V_J$ color diagram. The area defined by the solid line corresponds to our modified *BM*/*BX* criterion (see Sect. 3.1.2). **d)** IRAC colors of the MIPS sources located at $1.5 < z < 3$. The box illustrates the IRAC peaker selection criterion proposed by Huang et al. (2004). The typical uncertainties for each population are shown in the corners of the figures.

we applied the various criteria previously discussed to the MIPS-24 $\mu$m sample described in Sect. 2. We then analyzed the relative weight of the different subsamples of 24 $\mu$m sources identified with the *BzK*, *BM*/*BX*, and IRAC peaker selections with respect to the whole population of 24 $\mu$m-selected galaxies.

Our results are illustrated in the different panels of Fig. 2. On one hand, Fig. 2a shows the redshift distributions associated with our three UV/optical selections and compared to the redshift distribution obtained for the entire 24 $\mu$m source population in COSMOS. On the other hand, Figs. 2b–d represent the corresponding color diagrams along with the distribution of the 24 $\mu$m sources independently identified in the redshift range associated to each selection ($1.4 < z < 2.5$ for the *BzK* selection, $1.4 < z < 2.8$ for our modified *BM*/*BX* criterion, and $1.5 < z < 3$ for the IRAC peakers) using our redshift identifications from the catalog of Ilbert et al. (2009). The uncertainties characterizing the photometric redshifts of the 24 $\mu$m galaxy population in COSMOS have been thoroughly discussed by Le Floc'h et al. (2009) and Ilbert et al. (2009). Even at $1 < z < 3$, they are substantially smaller than the typical redshift range where the color selections operate ($1\sigma_z < 0.15$ up to $i^+_{AB} < 25$ mag and $z < 3$), so they should not affect our final conclusions. Not surprisingly, we see that the distributions characterizing the *BzK*, *BM*/*BX*, and IRAC peaker subsamples generally cover the redshift range of $1 < z < 3$, as expected from the definition of their associated selections. Nonetheless, these distributions clearly show that some of the criteria present substantial biases. Hereafter, we discuss the redshift properties characterizing each individual subsample in more detail.

- *BzK galaxies*: out of the 7227 MIPS sources lying in the redshift range $1.4 < z < 2.5$, we found that 6623 objects satisfy the *BzK* criterion. This represents 92% of the whole MIPS population at these redshifts, implying that the *BzK* selection is particularly efficient and weakly affected by dust obscuration. This high efficiency can be explained by the parallel evolution in the *BzK* diagram of the extinction vector to the line defining the *BzK* criterion for star-forming galaxies ($BzK = -0.1$), hence allowing selection of deeply obscured sources provided they are detected in the *K*-band.

Furthermore, the redshift distribution (Fig. 2a) reveals that the presence of contaminants at $z < 1.4$ is clearly negligible, while the $BzK$ colors of the MIPS sources identified in the $1.4 < z < 2.5$ redshift range (based on photometric redshifts) but not selected as $BzK$ sources are distributed very close below the threshold of $BzK = -0.1$ (see Fig. 2b). It shows that the small incompleteness of the $BzK$ selection at $1.4 < z < 2.5$ could simply result from optical/near-IR photometric uncertainties that are spreading sources below the borderline of the criterion, as well as small uncertainties in the photometric redshifts of sources close to the redshift boundaries of the selection. As an interesting aside, we also note that 84% of the MIPS sources with $2.5 < z < 3$ are still selected as $BzK$ sources. It suggests that the $BzK$ criterion could also be applied successfully at even higher redshift, at least for our sample of dusty luminous galaxies.

It is important to stress that the high success rate of identifications that we find with the $BzK$ technique is largely due to the depth of the optical and near-IR observations available in the COSMOS field. Several high-redshift 24 $\mu$m galaxies are indeed associated with faint optical/near-IR counterparts, and the ratio of MIPS sources identified with the $BzK$ selection would have been much lower if we had used shallower data at optical and near-IR wavelengths. As an example we restricted the COSMOS $K_s$-band sample to $K_s = 22$, $K_s = 22.5$ and $K_s = 23$, and we found that with these additional cuts only 42%, 72%, and 89% of the MIPS population at $1.4 < z < 2.5$ would have been identified with the $BzK$ selection. Given the large contribution of dusty luminous galaxies to the cosmic star formation density at $z \sim 2$ (e.g., Caputi et al. 2007; Rodighiero et al. 2010), this clearly illustrates the critical need for deep near-IR observations when probing the star-forming high-redshift galaxy population with the $BzK$ criterion.

Finally, we also recall that 4% of the sources from the very first sample of 24 $\mu$m detections extracted from the MIPS imaging of COSMOS (see Sect. 2) could not be matched with the optical catalog of Ilbert et al. (2009). We then have no information on their colors and their redshift. Given their faintness at short wavelengths, these galaxies most probably lie at $z > 1$. If they were all located at $1.4 < z < 2.5$, they would represent 15% of the whole population of 24 $\mu$m sources identified in this redshift range. The fraction of MIPS sources selected as $BzK$ galaxies would thus decrease from 92% down to ~78%.

- *BM/BX sources*: the distribution shown in Fig. 2a reveals that the $BM/BX$ criterion enables identification of dusty galaxies in the redshift range expected from the analysis that we presented in Sect. 3.2, but with a much lower efficiency than the $BzK$ and the IRAC peaker selections. Out the 7459 MIPS sources with $1.5 < z < 2.8$, only 3754 (i.e., ~50%) are indeed identified as $BM/BX$ galaxies. To understand the origin of this bias we illustrate in Fig. 2c the distribution of the 24 $\mu$m sources at $1.5 < z < 2.8$ in the $BM/BX$ diagram. It clearly shows that many of them are located outside of the $BM/BX$ selection area that we defined earlier, because of much redder colors than observed on average in the optical sample selected at $1.5 < z < 2.8$. Over this redshift range, the comparison between the $BM/BX$ properties of the MIPS sources and that of the COSMOS $i^+$-band selected population displayed in Fig. 1 is in fact particularly striking. According to the galaxy tracks represented in this figure, the MIPS sources located on the right-hand side of the $BM/BX$ selection box correspond either to galaxies with substantial extinction ($E(B-V) > 0.2$) or to lower redshift contaminants that we could have falsely identified with high-redshift objects. The latter is however unlikely given how few catastrophic failures there are among the photometric redshifts of the MIPS-selected population in COSMOS (Ilbert et al. 2009; Le Floc'h et al. 2009), along with the excellent agreement that we just found between the $BzK$ selection and the MIPS sample at $z \sim 2$. Therefore we conclude that the large number of 24 $\mu$m sources missed by the $BM/BX$ selection correspond to galaxies truly located at $1.5 < z < 2.8$ but strongly reddenned by dust extinction. This is obviously not surprising since the *Spitzer* mid-IR observations naturally favor the selection of dusty objects. Nevertheless it clearly reveals how the $BM/BX$ criterion is biased toward identifying UV-bright sources with little or no dust obscuration ($E(B-V) < 0.2$) and how this selection can thus miss a large number of luminous dust-enshrouded galaxies in the distant Universe. In Sect. 5 we quantify the impact of this bias in more detail on the bright end of the IR LF of star-forming galaxies at $z \sim 2$.
- *IRAC peakers*: among the 7755 MIPS sources located at $1.5 < z < 3$, a total of 4942 galaxies were selected as IRAC peakers. This corresponds to an average completeness of ~64% over this redshift range, showing that this criterion is also suited to distant galaxies but slightly less efficient than the $BzK$ selection. This lower efficiency must come from other effects than dust extinction since the IRAC criterion is based on data taken at longer wavelengths. A possible explanation is that the color selection of IRAC peakers has been restricted to identifying only those galaxies where the stellar bump is particularly pronounced, while dusty objects usually show a wider diversity of SEDs in the near-IR given the combined effect of stellar and hot dust emission. Besides this, the COSMOS photometric uncertainties in the IRAC bands are typically greater than those obtained at shorter wavelengths (e.g., Ilbert et al. 2009). As we can see in Fig. 2d this may result in distributing galaxies at $1.5 < z < 3$ over a slightly wider range of IRAC colors while increasing the contamination from galaxies at lower redshifts. Indeed we note that the redshift distribution of the 24 $\mu$m sources identified as IRAC peakers extends below $z \sim 1.5$, with 23% of the subsample located at $1 < z < 1.5$. Finally, although bright X-ray AGNs were removed from our initial sample, we cannot fully exclude a residual contamination from high-redshift, obscured nuclei detected at 24 $\mu$m. Their SED is usually characterized by a rising featureless, hot dust continuum, which can totally outshine the stellar emission of the galaxy when the AGN is luminous enough (Brand et al. 2006; Menéndez-Delmestre et al. 2009; Desai et al. 2009). In this case their hosts exhibit much redder colors than those allowed by the "IRAC peaker" selection, which would contribute to lowering its efficiency. However, the AGN contribution to the whole population of IR galaxies and to the cosmic infrared background is likely not more than 15% (e.g., Jauzac et al. 2011), so their possible contamination in our sample can not be the main explanation for the incompleteness of the IRAC peaker method.

### 4.2. Infrared-luminous sources with optically-faint counterparts at $z \sim 2$

In the analysis presented in the previous subsection we have seen that a substantial fraction of the high-redshift, mid-IR selected galaxies are strongly reddened by dust extinction, and they can

thus be missed when purely relying on rest-frame UV color selection techniques. Conversely, the selection of distant sources characterized by a large excess of IR emission such as the OFIR objects will necessarily be biased *against* dust-free galaxies. To quantify this effect, we applied the optical/mid-IR criterion described in Sect. 3.2 to our MIPS galaxy sample using the $r^+$-band observations of COSMOS and extended this criterion down to $F_{24\,\mu m} = 0.08$ mJy in order to probe a wider range of mid-IR luminosities. In Fig. 3a we show the distribution of the $r^+ - [24]$ colors for the MIPS-selected sources as a function of redshift, which confirms that most of the OFIR galaxies satisfying the criterion of Dey et al. (2008) are indeed located at $1.5 < z < 3$. Figures 3b, c illustrate the corresponding redshift distributions obtained for MIPS sources with $F_{24\,\mu m} > 0.08$ mJy and $F_{24\,\mu m} > 0.3$ mJy, respectively, compared to the distribution of the full MIPS-selected sample in COSMOS. The OFIR sources only represent ~30% (2350 sources on the 7755 sources with $1.5 < z < 3$) of the population of MIPS galaxies selected with $F_{24\,\mu m} > 0.08$ mJy at $1.5 < z < 3$, but as we see in the next section their contribution is rising with the mid-IR luminosity. Above a 24 $\mu$m flux of 0.3 mJy, their fraction reaches ~60% of the 24 $\mu$m-selected population at $z \sim 2$.

The fact that the fraction of galaxies with 24 $\mu$m to optical-band flux ratios satisfying Eq. (4) rises as a function of 24 $\mu$m flux is not an artificial selection effect due to the relative depths of our MIPS and $r^+$-band COSMOS observations. Even at the 24 $\mu$m flux limit of 0.08 mJy the optical COSMOS data are deep enough to identify galaxies as red as the color threshold used in the criterion proposed by Dey et al. (2008). Also it implies that the 4% of the initial 24 $\mu$m detections that we could not identify at optical and near-IR wavelengths (Sect. 2) satisfy Eq. (4) independently of their mid-IR flux density. Since these extremely red colors are unlikely associated to galaxies at $z < 1$ (see Fig. 3a) the relative contribution of galaxies selected at $1.5 < z < 3$ with this criterion could reach ~45% at $F_{24\,\mu m} > 0.08$ mJy.

As we already argued, this selection of high-redshift galaxies based on extremely red mid-IR/optical colors is by construction biased toward dust-obscured sources with very faint optical luminosities. For example, we found that 66% of these objects have $r^+ > 26$ mag while the $r^+$-band magnitude distribution of the MIPS sources with $1.5 < z < 2.8$ peaks at $r^+ \sim 25$ mag (only 21% of them have $r^+ > 26$ mag). Although they do not represent a dominant population in terms of source density, this nicely illustrates the contribution of luminous high-redshift, star-forming galaxies that may be missed by optical surveys because of dust obscuration. In fact, 65% of the OFIR sources have an extinction of $E(B-V) \geq 0.4$ according to the optical SED fitting of Ilbert et al. (2009), while this percentage decreases to only 44% for the whole population of MIPS sources in the same redshift range. Furthermore, galaxies selected with this technique differ dramatically from those identified with the $BM/BX$ selection, which we found to be strongly biased *against* dusty high-redshift galaxies. In Fig. 4 we compare the distribution of the OFIR sources in the $BzK$ diagram with the distribution of galaxies selected with our modified $BM/BX$ criterion. The overlap between the two subsamples is relatively small as only 8% of the MIPS sources at $1.5 < z < 2.8$ satisfy the two selection criteria, and not surprisingly the OFIR objects are characterized by much redder colors than the $BM/BX$ sources. Since the OFIR galaxies and the $BM/BX$-selected sources share very similar redshift distributions (compare Figs. 2a and 3b) and given the extinction vector at $z \sim 2$ in the $BzK$ diagram (Fig. 4), the lack of overlap between these two populations is mostly the effect of dust extinction.

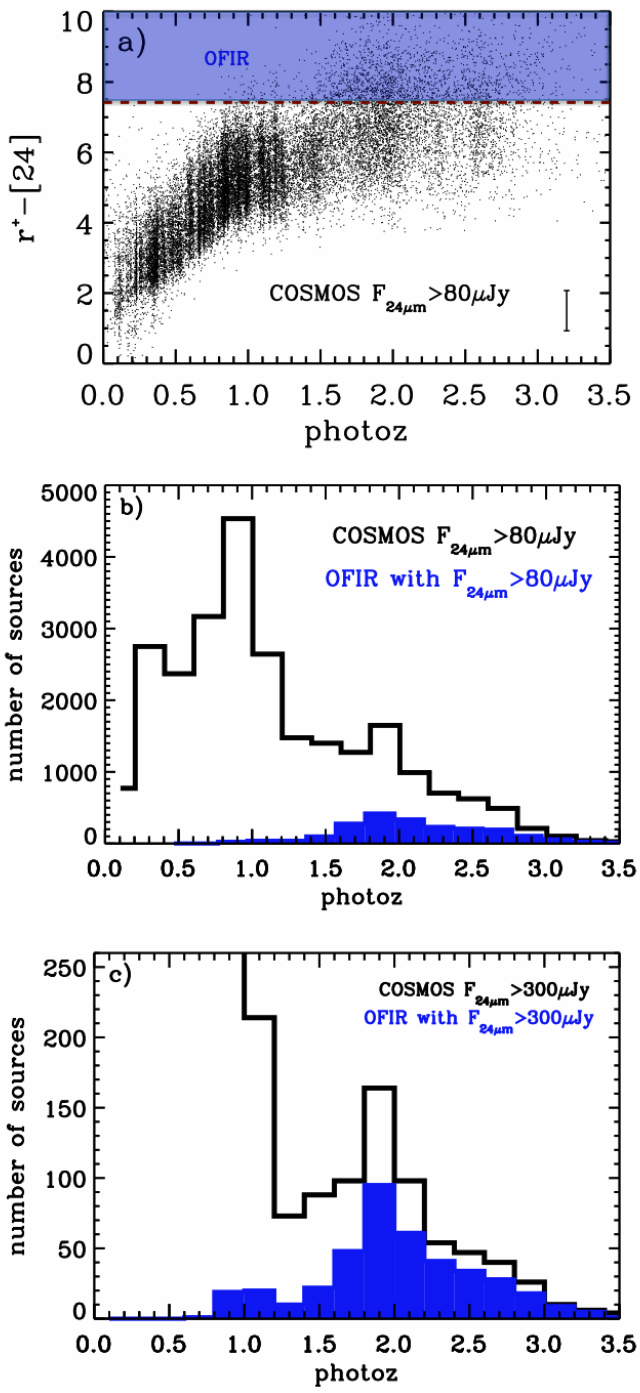


**Fig. 3. a)** The $r^+ - [24]$ color distribution of the MIPS 24$\mu$m sources as a function of redshift in the COSMOS field. Galaxies selected as OFIR sources are characterized by $r^+ - [24]$ colors redder than the threshold indicated by the dashed line. This criterion effectively selects galaxies at $1.5 < z < 3$. The typical uncertainties on the $r^+ - [24]$ color have been calculated at $1.5 < z < 3$ and are shown in the right corner. **b)** Redshift distribution of the OFIR galaxies with $F_{24\,\mu m} > 0.08$ mJy (blue filled histogram) compared to the redshift distribution obtained for the full MIPS-selected galaxy population in COSMOS (black solid line). **c)** Redshift distributions derived from the MIPS sample restricted to sources with $F_{24\,\mu m} > 0.3$ mJy (same color definitions as in **(b)**). The relative contribution of the OFIR galaxies at $1.5 < z < 3$ increases with mid-IR luminosities.

In Fig. 5 we illustrate in a more quantitative way how the OFIR objects and the other selections overlap with each other.

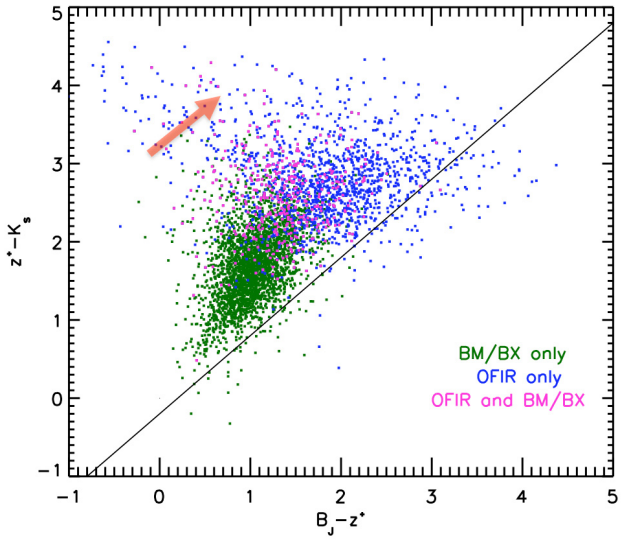


**Fig. 4.** Distribution of the 24 $\mu$m sources selected as OFIR galaxies (blue dots) and with the *BM*/*BX* criterion (green dots) in the *BzK* diagram. Only sources at $1.5 < z < 2.8$ are represented, and galaxies satisfying the two selections are shown in pink. The OFIR sources are characterized by redder colors, most likely due to higher dust extinction. The red arrow represents the extinction vector.

Since we found that the high efficiency of the *BzK* criterion is maintained up to $z \sim 3$ (at least when applied to our mid-IR sample, see Sect. 4.1), we compared our different selections over the widest possible redshift range (i.e., $1.5 < z < 2.8$) to minimize the statistical uncertainties. More than half of the population of OFIR sources are also selected as IRAC peakers indicating that an important part of the sources presenting extreme MIR color excess have an SED dominated by the stellar bump.

## 5. Galaxy 8 $\mu$m luminosity function and star formation rate density at $z \sim 2$

In the two previous sections we described a number of color selection techniques that have been widely used for identifying star-forming galaxies at $1.5 < z < 3$, and we quantified their respective contribution to the total number density of MIPS-selected high-redshift sources in order to estimate the bias that these selections suffer because of dust extinction. We want to extend this analysis by measuring the mid-IR LF of the different subsamples of galaxies selected based on these techniques, so as to infer their contribution to the total IR luminosity density of the Universe and the cosmic star formation rate density observed at $z \sim 2$. Here we explain the methods used to obtain the 8 $\mu$m rest-frame LF, the IR luminosity density and the SFR.

### 5.1. 8 $\mu$m luminosity function

The galaxy LFs were all computed at rest-frame 8 $\mu$m. The redshift distributions of the sources selected with the techniques described earlier mostly peak at $z \sim 2$ (Figs. 2a and 3b) and at these redshifts the measure of 8 $\mu$m luminosities ($L_{8\,\mu\mathrm{m}}$) based on 24 $\mu$m fluxes is therefore almost independent of the SED templates assumed for deriving the *k*-corrections. Also, the 8 $\mu$m luminosity of star-forming galaxies mostly originates from the emission of the 7.7 $\mu$m and 8.6 $\mu$m polycyclic aromatic hydrocarbon (PAH) lines, which represent the most prominent features in the mid-IR spectrum of dusty galaxies (e.g., Laurent et al. 2000; Dale et al. 2001; Brandl et al. 2006; Smith et al. 2007). These features are stochastically heated by the radiation field of young stellar populations, and as it was demonstrated by numerous studies of local sources, their luminosity is tightly correlated with the total Infrared luminosity of galaxies, and therefore with their SFR (e.g., Roussel et al. 2001; Wu et al. 2005; Brandl et al. 2006; Calzetti et al. 2007; Díaz-Santos et al. 2008; Goto et al. 2011). Furthermore, observations of distant sources with *Spitzer* and more recently with *Herschel* have revealed that this correlation between the 8 $\mu$m and the total IR luminosity of star-forming galaxies extends up to at least $z \sim 2$ (Pope et al. 2008; Rigby et al. 2008; Bavouzet et al. 2008; Menéndez-Delmestre et al. 2009; Elbaz et al. 2011), suggesting that the 8 $\mu$m emission is a fairly good tracer of star-forming activity also in high-redshift galaxies.

To convert the observed MIPS-24 $\mu$m fluxes into luminosities at 8 $\mu$m we used the library of IR SED templates of Chary & Elbaz (2001). In this library the galaxy IR SEDs vary as a function of total IR luminosity ($L_{\mathrm{IR}} = L_{8-1000\,\mu\mathrm{m}}$) and for a given redshift the flux density measured at 24 $\mu$m corresponds to a unique monochromatic luminosity at any IR wavelengths. However we stress again that for our current analysis the *k*-corrections only depend on the shape of these templates between $\lambda_0 = 8$ $\mu$m and $\lambda_1 = 24\ \mu\mathrm{m}/(1+z)$. At $z \sim 2$ they are thus barely sensitive to the choice of SEDs and do not depend on the uncertainties that have been shown to affect the extrapolations of mid-IR fluxes to total IR luminosities (Elbaz et al. 2010). In fact we computed the rest-frame 8 $\mu$m luminosities of the MIPS galaxy sample using the libraries of IR SED templates proposed by Dale & Helou (2002), Lagache et al. (2004) and Rieke et al. (2009), and we found virtually no difference with the results obtained with the library of Chary & Elbaz (2001). This effect will be discussed in more details in a forthcoming paper by Le Floc'h et al. (in prep.) on the evolution of the mid-IR LF in COSMOS.

Based on these 8 $\mu$m luminosities we computed the LFs associated with our different subsamples over the $1.7 < z < 2.3$ redshift range and we compared these results to the global LF obtained at the same redshifts from the full sample of MIPS sources in COSMOS. These LFs are illustrated in the top panel of Fig. 6. They were estimated using the $1/V_{\mathrm{max}}$ method (Schmidt 1968), which is advantageous in two ways: no hypothesis on the shape of the LF is needed and the LF is directly measured from the observations. For each object we estimated the maximum comoving volume where it can be detected within our given redshift bin ($1.7 < z < 2.3$) using $V_{\mathrm{max}} = V_{z\mathrm{max}} - V_{z\mathrm{min}}$, where $z_{\mathrm{min}} = 1.7$ and $z_{\mathrm{max}}$ is the smallest value between the redshift bin upper limit ($z = 2.3$) and the redshift until which the source could be observed considering the 24 $\mu$m flux limit of our survey (i.e., $F_{24\,\mu\mathrm{m}} = 0.08$ mJy). The uncertainties on the determination of the LFs were estimated from the Poisson noise associated to the number of sources detected in each bin of luminosity. Since we are only interested in quantifying the relative contribution of galaxies identified with the color selection techniques discussed earlier as a function of mid-IR luminosity, we neglected the effect of other uncertainties like the 24 $\mu$m flux errors and the cosmic variance.

### 5.2. Star formation rate estimates and SFR density

Because the mid-IR emission of star-forming galaxies originates from dust features heated by ionizing photons coming from young stars, their mid-IR luminosity correlates pretty well

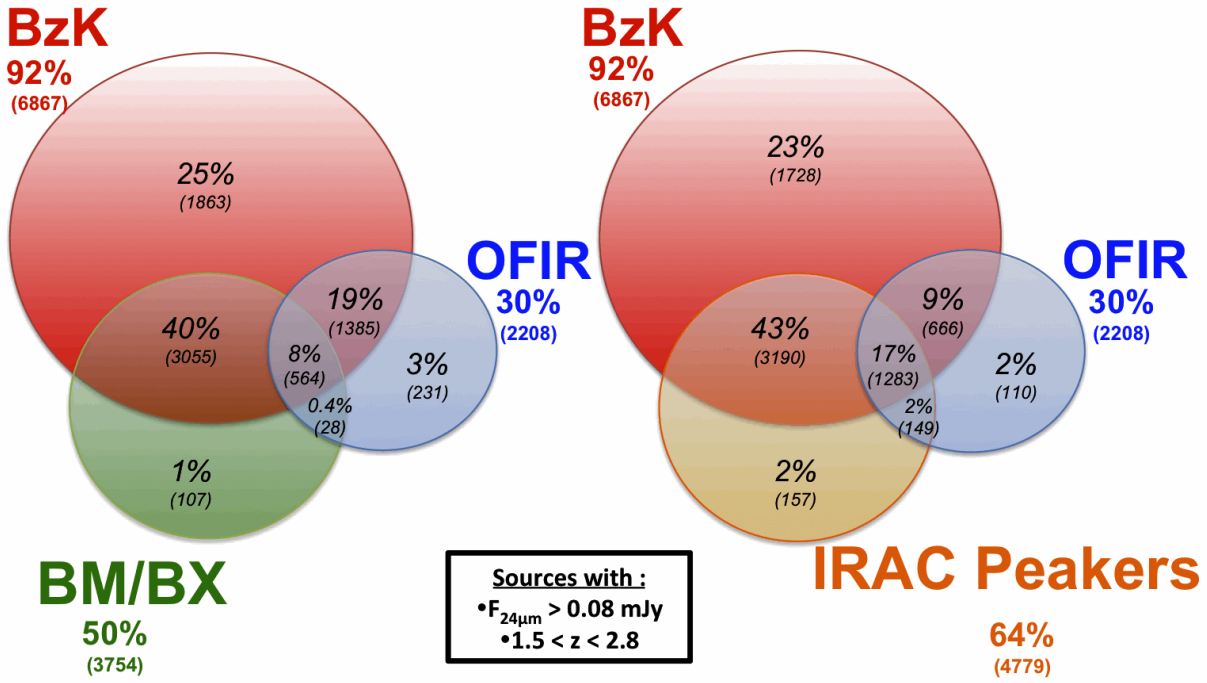


**Fig. 5.** Overlap between the populations of 24 $\mu$m sources with $F_{24\ \mu m} > 0.08$ mJy on the redshift range $1.5 < z < 2.8$. The percentages in bold are related to the total number of sources selected by the criterion considered. The percentages in italic correspond to the overlap between the populations. *Left*: overlap between the $BzK$, the $BM/BX$, and the OFIR sources. *Right*: overlap between the $BzK$, the OFIR sources, and the IRAC peakers.

with their SFR (e.g., Roussel et al. 2001; Förster Schreiber et al. 2004; Wu et al. 2005). For example Calzetti et al. (2007) and Díaz-Santos et al. (2008) analyzed the mid-IR properties of HII regions taken from a sample of local star-forming sources. They establish a significant correlation with a logarithmic slope ~1 between their 8 $\mu$m luminosity surface density corrected for stellar contribution and their luminosity measured from the Pa$\alpha$ emission line corrected for extinction. Similarly, the combination of the mid-IR and far-IR observations of the nearby Universe conducted with IRAS, ISO, *Spitzer* and AKARI revealed a tight relationship between $L_{8\ \mu m}$ and the total IR luminosity of local galaxies (e.g., Bavouzet et al. 2008; Goto et al. 2011). The deepest observations of the sky undertaken with *Herschel* have recently shown that this correlation extends up to at least $z \sim 3$ (Elbaz et al. 2011) and it may thus represent a universal property shared among star-forming galaxies at all cosmic times.

The relation obtained by Elbaz et al. (2011) between $L_{8\ \mu m}$ and the total infrared luminosity is linear ($L_{IR}/L_{8\ \mu m} \sim 4.9 \pm 0.2$ dex). Assuming the standard conversion inferred by Kennicutt (1998) between the $L_{IR}$ and the SFR ($SFR\,[M_\odot\ \mathrm{yr}^{-1}] = 1.72 \times 10^{-10}\ L_{IR}[L_\odot]$), we then obtain

$$SFR(M_\odot\ \mathrm{yr}^{-1}) = 8.4^{+4.9}_{-3.1} \times 10^{-10} L_{8\ \mu m}(L_\odot). \quad (5)$$

At the typical 8 $\mu$m luminosities found in our high-redshift sample (i.e., $L_{8\ \mu m} \sim 10^{11}$–$10^{12}\ L_\odot$), this is fully consistent with the relation we would get by combining the correlation measured by Goto et al. (2011) with the calibration from Kennicutt (1998):

$$SFR(M_\odot\ \mathrm{yr}^{-1}) = (34 \pm 9) \times 10^{-10} \times (L_{8\ \mu m}/L_\odot)^{0.94}. \quad (6)$$

Similarly, it agrees with the conversion we would obtain by applying the relationship from Calzetti et al. (2007) to a typical star-forming disk (i.e., 2–5 kpc in diameter) and assuming a case B recombination for converting the Pa$\alpha$ luminosity into a $SFR[M_\odot\ \mathrm{yr}^{-1}]$ of $6.79 \times 10^{-41}\ L_{Pa\alpha}[\mathrm{erg\ s}^{-1}]$, (Osterbrock & Bochkarev 1989; Alonso-Herrero et al. 2006). This last approach relies on the assumption for the size of the emitting region, but in the range of 8 $\mu$m luminosities that we measured, this effect is overwhelmed by the internal dispersion found in our sample and the uncertainty affecting the slope of the correlation between the Pa$\alpha$ and the 8 $\mu$m luminosity surface densities (Calzetti et al. 2007; Díaz-Santos et al. 2008; see also Alonso-Herrero et al. 2006). This relation is also consistent with the Pa$\alpha$ and the 8 $\mu$m luminosities that were recently measured in a submillimeter, lensed galaxy at $z \sim 2.5$ by Papovich et al. (2009). It suggests that it could still be applied to high-redshift sources even though it was derived from observations of the nearby Universe.

Given the good agreement between these different relationships, we thus inferred the total IR luminosity and SFR of the COSMOS MIPS sources using the linear relation obtained by Elbaz et al. (2011), as well as our Eq. (5), baring in mind that the other possible methods would have led to very similar results. Based on these determinations of $L_{IR}$ and SFR, we computed the contributions of the different populations of MIPS-selected sources discussed in Sect. 3 to the IR luminosity density of the Universe and the cosmic SFR density in three redshift bins: $1.5 < z < 1.9$, $1.9 < z < 2.3$ and $2.3 < z < 2.7$. To reach this goal we derived LFs in a similar way to the method described in Sect. 5.1, and we integrated the LFs above the luminosity corresponding to the 24 $\mu$m flux limit of our survey ($F_{24\ \mu m} = 0.08$ mJy) at the median of each redshift bin. Since we only aim at determining how the various galaxy subsamples *detected* with MIPS contributed to the total SFR density, we did not assume any extrapolation of the MIPS-selected source population to the faint end of the LF. Our results are shown in Fig. 7, which also illustrates the evolution of the total IR luminosity density inferred by Rodighiero et al. (2010) up to $z \sim 2.5$

and the cosmic star formation history compiled by Hopkins & Beacom (2006). The 1306 sources with no optical counterparts are obviously not taken into account here, but we have already seen that they contribute only a small fraction of the total number of galaxies identified in the COSMOS field. Furthermore, most of these unidentified sources have low 24 $\mu$m fluxes close to the sensitivity limit of the COSMOS MIPS data. This implies that their contribution to the IR luminosity density is even less than their contribution to the number of mid-IR selected sources, and therefore the lack of identification for these sources cannot severely bias our results.

## 6. Discussion

### 6.1. Contributions to the IR luminosity function

The top panel of Fig. 6 illustrates the LFs associated with the MIPS sources identified with the four color-selection techniques described in Sect. 3, compared to the total 8 $\mu$m LF observed at $1.7 < z < 2.3$ in the COSMOS field. The latter is also compared with the 8 $\mu$m LFs obtained by Caputi et al. (2007) and Rodighiero et al. (2010) from the GOODS and SWIRE surveys, which show relatively good agreement with our estimates. Except for the selection of OFIR galaxies, our analysis seems to indicate that the number of MIPS high-redshift galaxies selected with the *BzK*, *BM*/*BX*, and IRAC peaker criteria does not critically depend on the 8 $\mu$m luminosity itself. To better illustrate this result, we reproduced the evolution of these fractions with $L_{8\ \mu\mathrm{m}}$ in the bottom panel of the figure. To increase the statistics we extended the redshift bin up to $1.5 < z < 2.8$, which corresponds to the widest redshift range where the efficiencies of our different color selections can be simultaneously compared with one another. We see again that the fractions of MIPS galaxies selected as *BzK* and *BM*/*BX* sources or as IRAC peakers are fairly constant over the range of 8 $\mu$m luminosities probed by the MIPS observations. They correspond to the average fractions we had already derived based on their number density and their redshift distribution.

While the absence of correlation between $L_{8\ \mu\mathrm{m}}$ and the fraction of *BzK* sources or IRAC peakers is not necessarily unexpected, the result that we find for the *BM*/*BX* galaxies may deserve further explanations. Indeed we attributed the bias observed in the *BM*/*BX* selection to the effect of dust extinction (see Fig. 2c). Given the global trend that exists between galaxy bolometric luminosities and the IR/UV luminosity ratio (e.g., Bell 2003), one could have expected some broad correlation between the 8 $\mu$m luminosity and the fraction of MIPS high-redshift sources missed by the *BM*/*BX* criterion. In the most luminous galaxies though, the reddening of the optical light does not correlate anymore with the dust obscuration measured by the excess of $L_{\mathrm{IR}}$ over $L_{\mathrm{UV}}$ (e.g., Goldader et al. 2002; Reddy et al. 2006). This can be understood, for instance, if on one hand the UV/optical emission originates in spatially-extended regions of star formation where dust grains follow a rather clumpy distribution, while on the other, the IR light predominantly comes from very compact and optically-thick regions close to the center of galaxies. Since the MIPS observations of COSMOS are only sensitive to the very bright end of the high-redshift galaxy LF, we are likely in this luminosity regime where the $E(B-V)$ extinction is not directly correlated with the level of star-forming activity, thereby explaining the lack of any trend between the IR luminosity and the ability to detect galaxies based on their $U_nGR$ colors. Finally, it is also possible that our result at the highest luminosities ($L_{8\ \mu\mathrm{m}} > 10^{12}\ L_{\odot}$) is slightly affected by some AGN contribution, which can become significant at bright 24 $\mu$m fluxes (e.g., Martínez-Sansigre et al. 2005; Houck et al. 2005; Brand et al. 2006). In particular, the blue continuum arising from unobscured type-1 quasars could potentially bias the *BM*/*BX* selection; however, the majority of the most IR-luminous AGNs in COSMOS have also been detected in the X-rays (Hasinger et al. 2007; Brusa et al. 2010). They have been removed from our initial sample and therefore they should not influence the various trends that we find in Fig. 6.

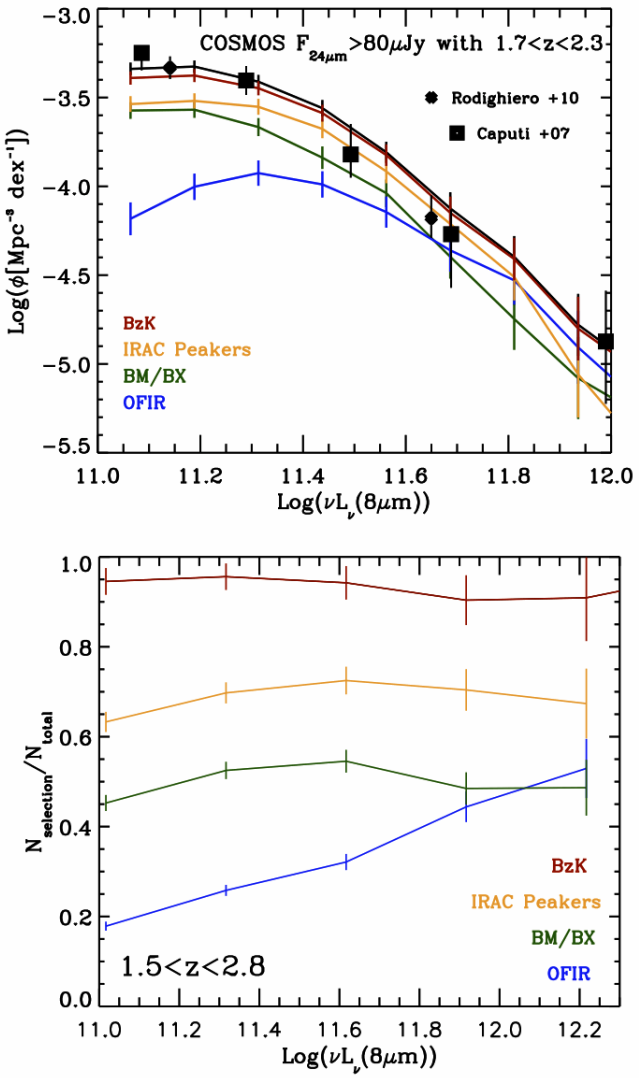


**Fig. 6.** *Top*: the 8 $\mu$m LFs of MIPS galaxies identified at $1.7 < z < 2.3$ with the color selection techniques described in Sects. 3 and 4 (red: *BzK*; green: *BM*/*BX*; yellow: IRAC peakers; blue: OFIR galaxies) compared to the total 8 $\mu$m LF measured in the COSMOS field (black solid line). Previous measurements of the total 8 $\mu$m LF at $z \sim 2$ by Rodighiero et al. (2010, filled diamonds) and Caputi et al. (2007, filled squares) are also shown for comparison. Error bars were estimated from the Poisson noise. *Bottom*: fraction of galaxies identified with each of the color selections as a function of $L_{8\ \mu\mathrm{m}}$ and in the $1.5 < z < 2.8$ redshift range. Color coding is similar to that used in *the top panel*.

Contrary to the behavior of the three rest-frame UV/optical selections, the percentage of OFIR galaxies clearly rises with IR luminosity. This is consistent with what we had qualitatively inferred from comparing their redshift distributions at $F_{24\ \mu\mathrm{m}} > 0.08$ mJy and $F_{24\ \mu\mathrm{m}} > 0.3$ mJy (see Fig. 3). In the previous section we argued that these sources are biased toward

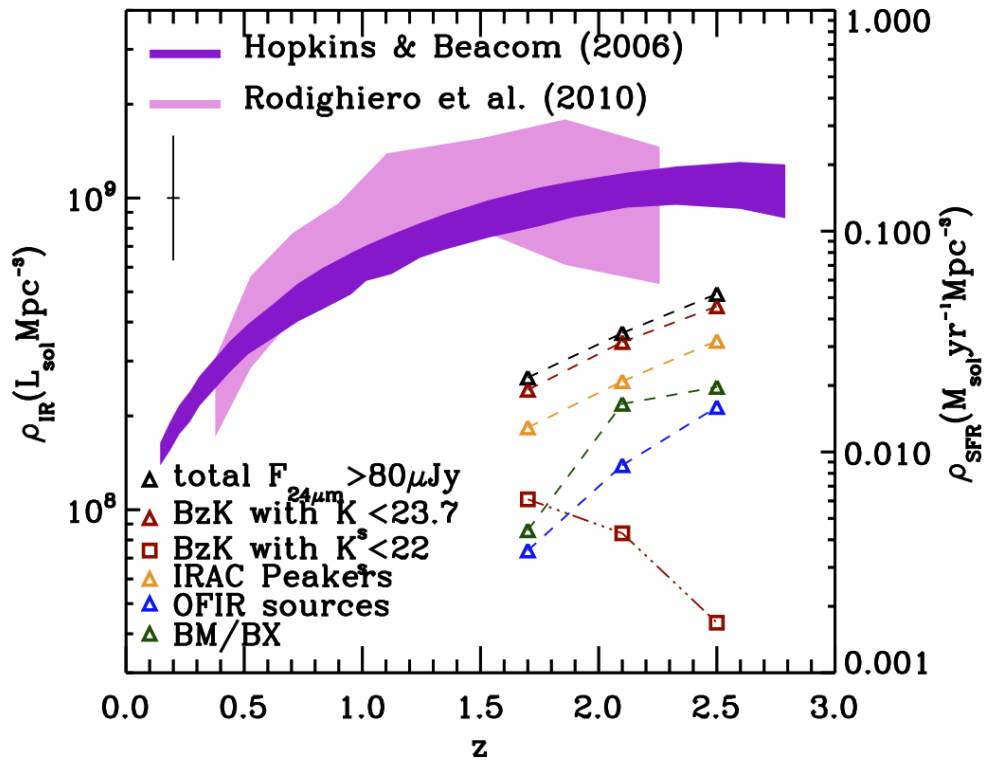


**Fig. 7.** Total infrared luminosity density produced at $1.5 < z < 1.9$, $1.9 < z < 2.3$ and $2.3 < z < 2.7$ by 24 $\mu$m sources with $F_{24\,\mu m} > 0.08$ mJy (black triangles), compared to the contribution of 24 $\mu$m sources identified with the selection techniques described in Sects. 3 and 4 (red: $BzK$; green: $BM/BX$; yellow: IRAC peakers; blue: OFIR galaxies with photo-$z$ identification). For galaxy samples where the MIPS 24 $\mu$m emission is mostly produced by star formation (i.e., $BzK$ and $BM/BX$ soursces, IRAC peakers) the IR luminosity density can be read as a star formation density (right vertical axis) assuming the conversion from Kennicutt (1998). For comparison, the evolution of the total IR luminosity density inferred by Rodighiero et al. (2010) up to $z \sim 2.5$ is illustrated by the lightly shaded region. The cosmic star formation history derived by Hopkins & Beacom (2006) is represented by the dark shaded area. The typical uncertainty affecting our estimates is shown by the vertical line in the top left corner of the diagram.

highly obscured galaxies. Assuming that dust extinction must correlate with the observed 24 $\mu$m/optical flux ratio of galaxies at $z \sim 2$, it could thus explain the trend that we find with luminosity. Furthermore, this trend could partly originate from an increasing contribution of obscured AGNs to the mid-IR luminosities of galaxies as a function of 24 $\mu$m flux (e.g., Brand et al. 2006; Menéndez-Delmestre et al. 2009). This rising contribution would boost their mid-IR emission with respect to their optical luminosity, hence leading to an $r^+ - [24]$ color satisfying the selection criterion of this population.

### 6.2. Implication for the cosmic star formation history

Even though we did not account for the contribution of galaxies below our 24 $\mu$m flux limit we see in Fig. 7 that star-forming galaxies detected in the COSMOS mid-IR survey contribute a substantial amount of the total IR luminosity density at $z \sim 2$, in agreement with previous findings (e.g., Caputi et al. 2007; Rodighiero et al. 2010). It implies that the incompleteness that affects the different color selection techniques previously described can result in non-negligible biases with respect to the global picture of galaxy evolution inferred from complete samples of high-redshift sources. For example we find that the MIPS sources selected with the $BM/BX$ criterion contribute only ~50% to the IR luminosity density produced by the galaxies with $F_{24\,\mu m} > 0.08$ mJy at $z \sim 2$. Similar to what is observed for the other color selections, this fraction is roughly constant over the whole $1.5 < z < 2.8$ redshift range. In the case of the $BM/BX$ technique we attributed this bias to the effect of dust extinction, and since the obscuration globally decreases with bolometric luminosity (Reddy et al. 2006) the incompleteness affecting this selection could probably be less if we had considered a deeper 24 $\mu$m selection. However, it is interesting to note that a very similar result has also been independently obtained by Guo & White (2009) with a semi-analytical approach and using the updated versions of the *Millenium Simulations* (Springel et al. 2005). According to the models they found that a large fraction of the total star formation density at $z \sim 2$ originates in galaxies that are too heavily obscured by dust to be selected with the $BM/BX$ criterion. In principle, incompleteness corrections can be applied to account for the difference between the properties of galaxies satisfying this color selection and the properties characterizing the underlying population of star-forming sources at these redshifts (e.g., Reddy et al. 2008). However, our analysis and the results from Guo & White (2009) reveal that a substantial extrapolation accounting for half of the most actively star-forming sources (i.e., $L_{8\,\mu m} > 10^{11.1}\,L_\odot$, corresponding to $SFR > 100\,M_\odot\,\mathrm{yr}^{-1}$) would be required to also take into account the large contribution of dusty luminous galaxies to the cosmic star formation density at $1.5 < z < 2.5$.

Similarly, we find that if the IRAC peaker selection is probably well suited to identifying of galaxies characterized by a pronounced stellar bump, it clearly cannot provide a complete view of the total contribution of massive star-forming sources to the

build-up of stellar mass at high redshift. Over the whole redshift range where this selection technique can be applied ($1.5 < z < 3$), up to ~30% of the total 8 $\mu$m luminosity density produced at the bright end of the LF is contributed by massive sources escaping the IRAC color criterion discussed previously. In the case of the OFIR sources, we find that this percentage can even go up to ~70%. Although the incompleteness affecting these two selections could be partly explained by the hot dust continuum of dust-obscured AGNs contributing to the rest-frame, near-IR emission of the most luminous (i.e., $L_{8\,\mu\mathrm{m}} > 10^{12}\ L_{\odot}$) galaxies at high redshift (e.g., Houck et al. 2005; Desai et al. 2009), it is unlikely to be the case for the majority of distant sources with more typical luminosities that are known to exhibit strong PAH features characteristic of star-forming activity at mid-IR wavelengths (Fadda et al. 2010). Furthermore, we recall the strong correlation that has been recently established between the 8 $\mu$m luminosity and the total IR luminosity of galaxies up to $z \sim 3$ (Elbaz et al. 2011), which reinforces the idea that the mid-IR luminosity characterizing the general galaxy population is mostly powered by star-forming activity. We thus conclude that a non-negligible fraction of the cosmic star formation density is missed by these two selection techniques.

On the other hand, we note that the $BzK$ approach enables an almost complete selection of star-forming galaxies at $z \sim 2$, at least in the range of luminosities that can be probed by our MIPS observations. This high level of completeness is observed not only for the bulk of the sample but also for the most luminous – and potentially the most highly obscured – galaxies. Using the optically-selected catalog of photometric redshifts in COSMOS (Ilbert et al. 2009), we verified that the reliability of the $BzK$ color criterion to select star-forming galaxies in the $1.4 < z < 2.5$ redshift range also remains valid at fainter luminosities. It suggests that this technique provides quite a powerful way to identify galaxies at this epoch of cosmic history, independently of the possibility of determining accurate photometric redshifts for these sources.

More generally speaking that a non-negligible fraction of high-z sources can be missed by optical color selections has also been observed by other groups using different kinds of analyses, and this bias likely comes not only from dust extinction but also from the broader diversity of high-redshift galaxy properties than was assumed in the definition of the color criteria explored so far. For instance, Ly et al. (2011) show that surveys of [OII] emitters can pick up a non-negligible number of $z \sim 1.5$ galaxies that are missed by the $BzK$ and $BM/BX$ techniques. Similarly, Caputi et al. (2011) found that, at $z = 3$–$4$, ~30% of the massive galaxies ($M \geq 10^{11}\ M_{\odot}$) would be missed by deep optical surveys, underlying the importance of deep near-IR surveys to supplement the identification of high-$z$ galaxies affected by extinction. Based on deep spectroscopy taken as part of the Vimos VLT Deep Survey, Le Fèvre et al. (2005) finally underlined that magnitude-selected samples provide a much more complete census of the high-redshift galaxy population than do color selection techniques. All these results converge in how the identifications of distant star-forming galaxies based on UV/optical color criteria result in a view of high-redshift star formation that cannot fully represent the global picture of galaxy evolution.

## 7. Summary and conclusions

Using the exquisite multi-wavelength imaging obtained in the COSMOS field, we analyzed the broad-band optical/near-IR colors and the photometric redshift distribution of a complete sample of distant ($1.5 < z < 3$) luminous galaxies selected at 24 $\mu$m with $F_{24\,\mu\mathrm{m}} > 0.08$ mJy. To quantify how selection effects and incompleteness can bias the different color selection techniques often used for identifying populations of high-redshift star-forming sources (e.g., $BzK$, $BM/BX$ and "IRAC peaker" selections, OFIR objects), we measured the fraction of MIPS-24 $\mu$m galaxies satisfying these color criteria within the redshift range where each of them is expected to apply with high efficiency. We also derived reliable estimates of their rest-frame 8 $\mu$m luminosities with minimal effects from the $k$-correction, which allowed us to constrain their SFR and their contribution to cosmic star formation density. Our results can be summarized as follows:

1. The $BzK$ color criterion allows an almost complete (~90%) identification of 24 $\mu$m sources at $1.4 < z < 2.5$. The rate of these identifications does not change with IR luminosity, which suggests that this technique provides a highly reliable way of identifying distant galaxies independently of obscuration. This can be explained by the weak dependence of the $BzK$ variable ($BzK \equiv [z - K] - [B - z]$) on the effect of dust extinction at $z \sim 2$. However, we emphasize that the success rate of the $BzK$ selection strongly relies on the availability of deep imaging at optical and near-IR wavelengths. With a cut at $K_s = 22$ (AB), the contribution of $BzK$-identified galaxies to the IR luminosity density produced by sources with $F_{24\,\mu\mathrm{m}} > 0.08$ mJy would fall to ~40%.
2. We adapted the original $BM/BX$ criterion to the existing COSMOS optical photometry using the deep imaging obtained with the $u^*$-band, $V_J$-band and $i^+$-band filters. We found that up to 50% of the MIPS selected galaxies at $1.5 < z < 2.8$ are missed by this selection technique. We explain this result as the effect of dust extinction, which more strongly affects the rest-frame UV emission of galaxies and makes their SED redder than the typical blue colors for galaxies satisfying the $BM/BX$ criterion. This is consistent with the results recently obtained by Guo & White (2009) based on *Millenium simulations* (Springel et al. 2005), who found that a large amount of the cosmic star formation density probably originates from massive sources that are too heavily obscured by dust to be identified with the UV color selections. At the bright end of the bolometric LF, the extrapolations and incompleteness corrections usually applied to account for this bias must therefore be quite large and uncertain.
3. Up to ~30% of the IR luminosity density produced at $z \sim 2$ by sources brighter than 80 $\mu$Jy originates from galaxies that fail to be identified thanks to the spectral shape of their stellar bump feature at rest-frame 1.6 $\mu$m (i.e., the so-called "*IRAC peaker*" selection). For the brightest galaxies in the mid-IR, this effect could be explained by a strong contribution from dust-obscured AGNs to the near-IR emission observed in the IRAC bands. For the bulk of the population, though, this reflects the larger uncertainties affecting the IRAC photometry, as well as the wide diversity of near-IR SEDs characterizing dusty galaxies, thanks to the combined contribution of hot dust and stellar emission.
4. The selection of OFIR sources based on the $R - [24]$ color is meant to identify dusty galaxies at $1.5 < z < 3$. While this technique is efficient at the very bright end of the mid-IR LF where galaxies are characterized by extremely high 24 $\mu$m/optical flux ratios, the fraction of sources selected with this criterion rapidly decreases at fainter luminosities. Assuming the depth of the COSMOS MIPS survey

($F_{24\,\mu m} > 0.08$ mJy), we find that only ~25% of the IR luminosity density of the Universe at $z \sim 2$ is produced by galaxies with such extreme colors.

These results suggest that color selections of distant star-forming galaxies can be affected by substantial biases and incompleteness, and therefore they must be used with caution. Depending on the spectral features or the SED range that they are supposed to probe, these high-redshift selections are probably less subject to contaminants than when using photometric redshifts of modest quality if the latter are strongly affected by catastrophic failures at $z > 1$. However, we have shown that identifying distant galaxies solely from optical/IR color criteria will most often provide an incomplete view of the whole population of high-redshift star-forming sources, hence requiring large and uncertain extrapolations to account for their incompleteness. Complete identifications based on high-quality spectroscopic redshifts or accurate photometric redshifts thus appear the most reliable approach for probing the formation and the evolution of galaxies in a global and cosmological context.

*Acknowledgements.* It is a pleasure to acknowledge the contribution from all our colleagues in the COSMOS collaboration. More information on the COSMOS survey is available at http://www.astro.caltech.edu/cosmos. This work is based on observations made with the *Spitzer* Space Telescope, a facility operated by NASA/JPL. Financial supports were provided by NASA through contracts Nos. 1289085, 1310136, 1282612, and 1298231 issued by the Jet Propulsion Laboratory. We also want to warmly thank our referee for his/her critical review of the manuscript, as well as Tanio Díaz-Santos for useful discussions related to our work. We are finally grateful to Marc Sauvage for his help and for his useful and numerous comments.

## References

Adelberger, K. L., & Steidel, C. C. 2000, ApJ, 544, 218
Adelberger, K. L., Steidel, C. C., Shapley, A. E., et al. 2004, ApJ, 607, 226
Alonso-Herrero, A., Rieke, G. H., Rieke, M. J., et al. 2006, ApJ, 650, 835
Arnouts, S., Walcher, C. J., Le Fèvre, O., et al. 2007, A&A, 476, 137
Aussel, H., Cesarsky, C. J., Elbaz, D., & Starck, J. L. 1999, A&A, 342, 313
Austermann, J. E., Aretxaga, I., Hughes, D. H., et al. 2009, MNRAS, 393, 1573
Bavouzet, N., Dole, H., Le Floc'h, E., et al. 2008, A&A, 479, 83
Bell, E. F. 2003, ApJ, 586, 794
Bertoldi, F., Carilli, C., Aravena, M., et al. 2007, ApJS, 172, 132
Blain, A. W., Smail, I., Ivison, R. J., Kneib, J.-P., & Frayer, D. T. 2002, Phys. Rep., 369, 111
Brand, K., Dey, A., Weedman, D., et al. 2006, ApJ, 644, 143
Brandl, B. R., Bernard-Salas, J., Spoon, H. W. W., et al. 2006, ApJ, 653, 1129
Brusa, M., Zamorani, G., Comastri, A., et al. 2007, ApJS, 172, 353
Brusa, M., Civano, F., Comastri, A., et al. 2010, ApJ, 716, 348
Bruzual, G., & Charlot, S. 2003, MNRAS, 344, 1000
Calzetti, D., Armus, L., Bohlin, R. C., et al. 2000, ApJ, 533, 682
Calzetti, D., Kennicutt, R. C., Engelbracht, C. W., et al. 2007, ApJ, 666, 870
Capak, P., Aussel, H., Ajiki, M., et al. 2007, ApJS, 172, 99
Capak, P. L., Riechers, D., Scoville, N. Z., et al. 2011, Nature, 470, 233
Caputi, K. I., Lagache, G., Yan, L., et al. 2007, ApJ, 660, 97
Caputi, K. I., Cirasuolo, M., Dunlop, J. S., et al. 2011, MNRAS, 413, 162
Chary, R., & Elbaz, D. 2001, ApJ, 556, 562
Cimatti, A., Cassata, P., Pozzetti, L., et al. 2008, A&A, 482, 21
Coppin, K., Halpern, M., Scott, D., et al. 2008, MNRAS, 384, 1597
Daddi, E., Cimatti, A., Renzini, A., et al. 2004, ApJ, 617, 746
Dale, D. A., & Helou, G. 2002, ApJ, 576, 159
Dale, D. A., Helou, G., Contursi, A., Silbermann, N. A., & Kolhatkar, S. 2001, ApJ, 549, 215
Desai, V., Soifer, B. T., Dey, A., et al. 2009, ApJ, 700, 1190
Dey, A., Soifer, B. T., Desai, V., et al. 2008, ApJ, 677, 943
Díaz-Santos, T., Alonso-Herrero, A., Colina, L., et al. 2008, ApJ, 685, 211
Dickinson, M., Papovich, C., Ferguson, H. C., & Budavári, T. 2003, ApJ, 587, 25
Elbaz, D., Daddi, E., Le Borgne, D., et al. 2007, A&A, 468, 33
Elbaz, D., Hwang, H. S., Magnelli, B., et al. 2010, A&A, 518, L29
Elbaz, D., Dickinson, M., Hwang, H. S., et al. 2011, A&A, 533, A119
Elvis, M., Civano, F., Vignali, C., et al. 2009, ApJS, 184, 158
Fadda, D., Yan, L., Lagache, G., et al. 2010, ApJ, 719, 425
Fontana, A., Pozzetti, L., Donnarumma, I., et al. 2004, A&A, 424, 23
Förster Schreiber, N. M., Roussel, H., Sauvage, M., & Charmandaris, V. 2004, A&A, 419, 501
Franx, M., Labbé, I., Rudnick, G., et al. 2003, ApJ, 587, L79
Glazebrook, K., Abraham, R. G., McCarthy, P. J., et al. 2004, Nature, 430, 181
Goldader, J. D., Meurer, G., Heckman, T. M., et al. 2002, ApJ, 568, 651
Goto, T., Arnouts, S., Inami, H., et al. 2011, MNRAS, 410, 573
Grazian, A., Salimbeni, S., Pentericci, L., et al. 2007, A&A, 465, 393
Guo, Q., & White, S. D. M. 2009, MNRAS, 396, 39
Hainline, L. J., Blain, A. W., Smail, I., et al. 2009, ApJ, 699, 1610
Hasinger, G., Cappelluti, N., Brunner, H., et al. 2007, ApJS, 172, 29
Hopkins, A. M., & Beacom, J. F. 2006, ApJ, 651, 142
Houck, J. R., Soifer, B. T., Weedman, D., et al. 2005, ApJ, 622, L105
Huang, J., Barmby, P., Fazio, G. G., et al. 2004, ApJS, 154, 44
Huang, J., Faber, S. M., Daddi, E., et al. 2009, ApJ, 700, 183
Hughes, D. H., Serjeant, S., Dunlop, J., et al. 1998, Nature, 394, 241
Ilbert, O., Capak, P., Salvato, M., et al. 2009, ApJ, 690, 1236
Ilbert, O., Salvato, M., Le Floc'h, E., et al. 2010, ApJ, 709, 644
Jauzac, M., Dole, H., Le Floc'h, E., et al. 2011, A&A, 525, A52
Kennicutt, R. C. 1998, ARA&A, 36, 189
Lagache, G., Dole, H., Puget, J., et al. 2004, ApJS, 154, 112
Laurent, O., Mirabel, I. F., Charmandaris, V., et al. 2000, A&A, 359, 887
Le Fèvre, O., Paltani, S., Arnouts, S., et al. 2005, Nature, 437, 519
Le Floc'h, E., Pérez-González, P. G., Rieke, G. H., et al. 2004, ApJS, 154, 170
Le Floc'h, E., Papovich, C., Dole, H., et al. 2005, ApJ, 632, 169
Le Floc'h, E., Aussel, H., Ilbert, O., et al. 2009, ApJ, 703, 222
Lilly, S. J., Le Fèvre, O., Renzini, A., et al. 2007, ApJS, 172, 70
Lonsdale, C. J., Polletta, M. d. C., Omont, A., et al. 2009, ApJ, 692, 422
Lutz, D., Poglitsch, A., Altieri, B., et al. 2011, A&A, 532, A90
Ly, C., Malkan, M. A., Hayashi, M., et al. 2011, ApJ, 735, 91
Madau, P., Ferguson, H. C., Dickinson, M. E., et al. 1996, MNRAS, 283, 1388
Marleau, F. R., Fadda, D., Storrie-Lombardi, L. J., et al. 2004, ApJS, 154, 66
Martínez-Sansigre, A., Rawlings, S., Lacy, M., et al. 2005, Nature, 436, 666
McCracken, H. J., Capak, P., Salvato, M., et al. 2010, ApJ, 708, 202
Menéndez-Delmestre, K., Blain, A. W., Smail, I., et al. 2009, ApJ, 699, 667
Noeske, K. G., Faber, S. M., Weiner, B. J., et al. 2007, ApJ, 660, L47
Osterbrock, D. E., & Bochkarev, N. G. 1989, SvA, 33, 694
Papovich, C. 2008, ApJ, 676, 206
Papovich, C., Rudnick, G., Rigby, J. R., et al. 2009, ApJ, 704, 1506
Pope, A., Chary, R.-R., Alexander, D. M., et al. 2008, ApJ, 675, 1171
Reddy, N. A., Steidel, C. C., Fadda, D., et al. 2006, ApJ, 644, 792
Reddy, N. A., Steidel, C. C., Pettini, M., et al. 2008, ApJS, 175, 48
Rieke, G. H., Young, E. T., Engelbracht, C. W., et al. 2004, ApJS, 154, 25
Rieke, G. H., Alonso-Herrero, A., Weiner, B. J., et al. 2009, ApJ, 692, 556
Rigby, J. R., Marcillac, D., Egami, E., et al. 2008, ApJ, 675, 262
Rodighiero, G., Vaccari, M., Franceschini, A., et al. 2010, A&A, 515, A8
Roussel, H., Sauvage, M., Vigroux, L., & Bosma, A. 2001, A&A, 372, 427
Salpeter, E. E. 1955, ApJ, 121, 161
Salvato, M., Hasinger, G., Ilbert, O., et al. 2009, ApJ, 690, 1250
Sanders, D. B., Salvato, M., Aussel, H., et al. 2007, ApJS, 172, 86
Sawicki, M. 2002, AJ, 124, 3050
Schinnerer, E., Smolčić, V., Carilli, C. L., et al. 2007, ApJS, 172, 46
Schmidt, M. 1968, ApJ, 151, 393
Scoville, N., Abraham, R. G., Aussel, H., et al. 2007a, ApJS, 172, 38
Scoville, N., Aussel, H., Brusa, M., et al. 2007b, ApJS, 172, 1
Simpson, C., & Eisenhardt, P. 1999, PASP, 111, 691
Smail, I., Ivison, R. J., & Blain, A. W. 1997, ApJ, 490, L5
Smith, J. D. T., Draine, B. T., Dale, D. A., et al. 2007, ApJ, 656, 770
Sorba, R., & Sawicki, M. 2010, ApJ, 721, 1056
Springel, V., White, S. D. M., Jenkins, A., et al. 2005, Nature, 435, 629
Steidel, C. C., Adelberger, K. L., Giavalisco, M., Dickinson, M., & Pettini, M. 1999, ApJ, 519, 1
Steidel, C. C., Adelberger, K. L., Shapley, A. E., et al. 2003, ApJ, 592, 728
Steidel, C. C., Shapley, A. E., Pettini, M., et al. 2004, ApJ, 604, 534
Taniguchi, Y., Scoville, N., Murayama, T., et al. 2007, ApJS, 172, 9
Thompson, D., Beckwith, S. V. W., Fockenbrock, R., et al. 1999, ApJ, 523, 100
Wolf, C., Meisenheimer, K., Rix, H.-W., et al. 2003, A&A, 401, 73
Wu, H., Cao, C., Hao, C.-N., et al. 2005, ApJ, 632, L79
Yan, L., Chary, R., Armus, L., et al. 2005, ApJ, 628, 604